I. Device design and micro-nano fabrication

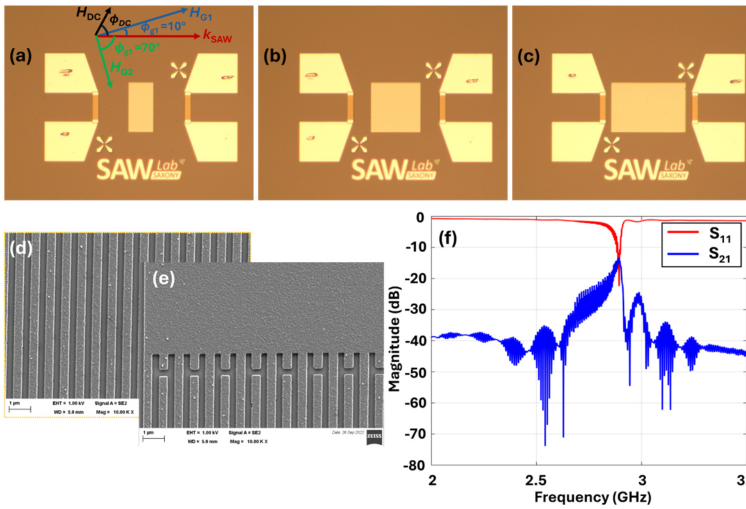

FIG 1. Low-loss, wideband, non-reciprocal magnetoacoustic RF isolator based on 2.87 GHz fundamental mode surface acoustic wave (SAW) driven non-reciprocal spin waves in the non-collinear dipolar-coupled FeGaB (20 nm)/SiO_2(5 nm) /FeGaB (20 nm) ferromagnetic stack. (a-c) Optical image of the wideband magnetoacoustic RF isolators with dipolar magnetic stack dimensions of (a) 100×300 μm^2, (b) 200×300 μm^2 and (c) 300×300 μm^2. The two FeGaB layers have non-collinear uniaxial anisotropy fields enabled by different *in-situ* growth field directions as shown in **Figure 1(a)** inset. A DC bias magnetic field H_{DC} is applied at φ_{DC} with respect to k_{SAW}. (d-e) **S**canning electron microscopy (SEM) images of ~300 nm wide interdigital transducers (IDTs) fingers. (f) RF probing measurements of the input reflection coefficient S_{11} and forward transmission coefficient S_{21} reveal a low insertion loss of ~13 dB and a minimum S_{11} of ~ –22 dB, indicating good impedance matching at the fundamental mode frequency of ~2.87 GHz.

Figure 1 shows optical images of low-loss, wideband non-reciprocal magnetoacoustic RF isolators. These devices consist of dipolar-coupled FeGaB (20 nm)/SiO_2 (5 nm)/FeGaB (20 nm) ferromagnetic stacks placed between input and output interdigital transducers (IDTs) on 128° Y-X cut $LiNbO_3$ substrates. The two FeGaB layers have distinct, non-aligned uniaxial anisotropy fields, induced by varying the in-situ 200 Oe magnetic field direction during deposition: the first layer at 10° and the second at 70° relative to the SAW propagation vector k_{SAW}, as illustrated in the inset of **Figure 1(a)**. A DC magnetic field at angle φ_{DC} is applied to tune non-reciprocal SAW–spin wave interactions, enabling wideband non-reciprocity. The non-collinear magnetic configuration can reduce insertion loss and broadens the non-reciprocal bandwidth [1]—key for low-power, full-duplex radar and radio communication applications [2]. The dipolar-coupled ferromagnetic stacks with dimensions of 100×300 μm², 200×300 μm², and 300×300 μm² were deposited by magnetron sputtering. The input and output aluminum IDTs (~2.87 GHz fundamental mode) were patterned using laser lithography, e-beam lithography, e-beam evaporation, and lift-off. The scaning electron microscopy (SEM) images confirm high-quality fabrication of ~300 nm wide IDT fingers. The fabricated magnetoacoustic device in **Figure 1(b)** exhibits a low insertion loss of ~13 dB at 2.87 GHz under RF probing measurements, significantly better than conventional magnetoacoustic devices (>40 dB loss) with higher-order SAW modes [3-7]. A minimum input reflection (S_{11}) of −22 dB indicates good impedance matching and low RF reflection. Forward transmission (S_{21}) displays ~10 MHz spaced modulation of the SAW resonance peak ("triple transit echoes"), likely from multiple reflections between IDTs, confirming low loss, strong magnitude and long propagation distance of fundamental SAW in the magnetoacoustic device.

II. Wideband magnetoacoustic absorption and non-reciprocity

S-parameters were measured under a DC magnetic field aligned with k_{SAW} to characterize magnetoacoustic absorption and non-reciprocity, enabled by strong coupling between non-reciprocal spin waves and the fundamental SAW mode. As shown in **Figure 2 (a)**, the 200×300 μm^2 non-collinear ferromagnetic stack exhibits ~40 dB forward absorption near the spin wave branches, with multiple wide absorption bands spanning 2.48–2.58 GHz, 2.62–2.92 GHz, 2.94–3.03 GHz, and 3.08–3.15 GHz. In contrast, backward absorption shows spin wave branches shifted to higher magnetic fields (**Figure 2(b)**), producing four wideband non-reciprocity branches with alternating polarity (**Figure 2(c)**). The maximum non-reciprocity reaches ~40 dB (200 dB/mm) near modulated SAW peaks, where standing wave formation enhances acoustic resonance—nearly 10× higher than the 22 dB/mm reported in earlier devices using 1425 MHz fifth-order SAWs [3, 4]. For the 300 × 300 μm^2 non-collinear stack, a more symmetric non-reciprocity profile is observed, likely due to variations in the uniaxial anisotropy fields caused by growth field inhomogeneity. Two dominant non-reciprocity bands appear at 2.62–2.92 GHz and 2.94–3.03 GHz, with a peak non-reciprocity of ~51 dB (170 dB/mm). Detailed S-parameters at four fields showing the widest positive or negative non-reciprocity bands are presented in

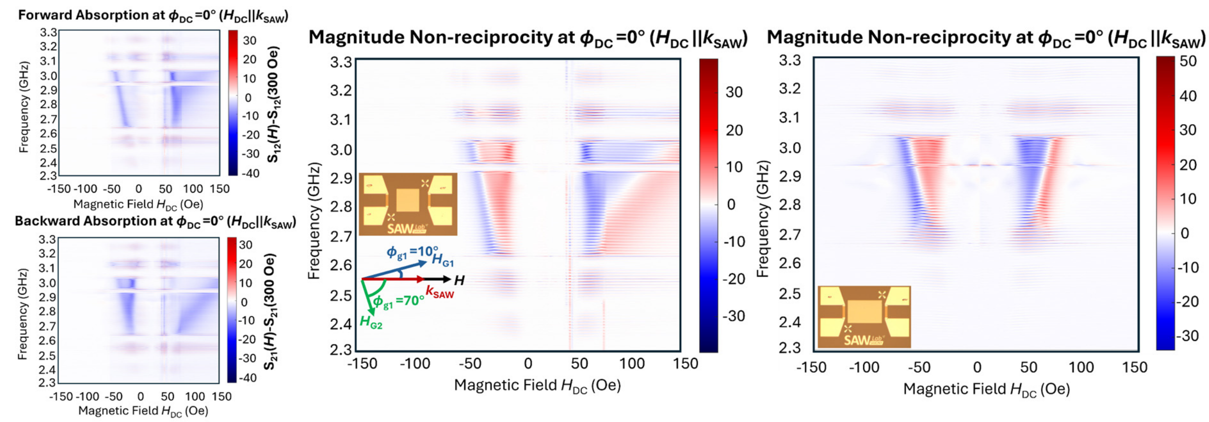

FIG 2. Wideband non-reciprocity of the non-reciprocal magnetoacoustic RF isolator based on the non-collinear dipolar-coupled ferromagnetic stack. (a) Forward Absorption $S_{21}(H)$-S_{21}(300 Oe) for the 200 μm×300 μm stack. (b) Backward Absorption $S_{12}(H)$-S_{12}(300 Oe) for the 200 μm×300 μm stack. (c) Magnitude non-reciprocity $S_{21}(H)$-$S_{12}(H)$ for the 200 μm×300 μm stack. Multiple wide non-reciprocity bands can be observed at 2.48–2.58 GHz, 2.62–2.92 GHz, 2.94–3.03 GHz, and 3.08–3.15 GHz. (d) Magnitude non-reciprocity $S_{21}(H)$-$S_{12}(H)$ for the 300 μm×300 μm stack. The non-reciprocity band is more symmetric compared with the 200 μm×300 μm stack, maybe due to different uniaxial anisotropy fields of the two layers from inhomegenity of growth magnetic field. Multiple wide non-reciprocity bands can still be observed at 2.62–2.92 GHz and 2.94–3.03 GHz.

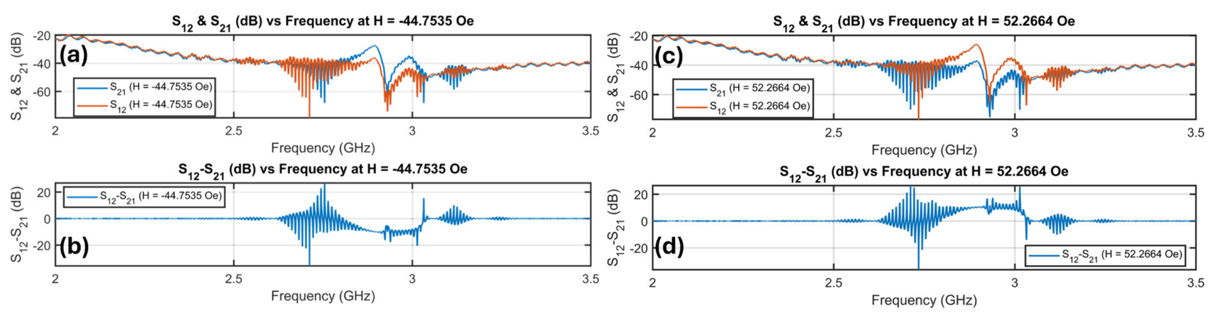

FIG 3. Forward transmission S_{21}, backward transmission S_{12} and non-reciprocity at magnetic fields leading to wideband non-reciprocity of the magnetoacoustic RF isolator based on the non-collinear ferromagnetic stack. The fields are non-symmetric to zero bias fields with opposite polarity of non-reciprocity. A maximum transmission of ~ −25 dB was realized at 2.87 GHz with ~10 dB non-reciprocity (33.3 dB/mm).

Figure 3. Notably, this wideband device demonstrates a maximum transmission of ~ −25 dB at 2.87 GHz with ~10 dB non-reciprocity (33.3 dB/mm), offering 40 dB higher transmission and 10 dB higher non-reciprocity than previous reports [3, 4]. The low-loss, high-absorption, wideband non-reciprocal magnetoacoustic isolator shows great potential for low power compact full-duplex radio/ radar commmunication system [2], efficient and coherent excitation of ground state NV^- centers [8] and non-reciprocal quantum information transfer platforms [9].

References

[1] L. Ushii, A. Slavin, and R. Verba, "Nonreciprocity of surface acoustic waves coupled to spin waves in a ferromagnetic bilayer with noncollinear layer magnetizations," *Phys Rev Appl,* vol. 22, no. 3, p. 034046, 2024.

[2] A. Nagulu and H. Krishnaswamy, "Non-magnetic non-reciprocal microwave components—State of the art and future directions," *IEEE Journal of Microwaves,* vol. 1, no. 1, pp. 447-456, 2021.

[3] P. J. Shah, D. A. Bas, I. Lisenkov, A. Matyushov, N. X. Sun, and M. R. Page, "Giant nonreciprocity of surface acoustic waves enabled by the magnetoelastic interaction," (in English), *Science Advances,* vol. 6, no. 49, 2020.

[4] D. A. Bas *et al.*, "Nonreciprocity of Phase Accumulation and Propagation Losses of Surface Acoustic Waves in Hybrid Magnetoelastic Heterostructures," (in English), *Phys Rev Appl,* vol. 18, no. 4, 2022.

[5] M. Huang *et al.*, "Large nonreciprocity of shear-horizontal surface acoustic waves induced by a magnetoelastic bilayer," *Phys Rev Appl,* vol. 21, no. 1, p. 014035, 2024.

[6] M. Küß, S. Glamsch, A. Hörner, and M. Albrecht, "Wide-band nonreciprocal transmission of surface acoustic waves in synthetic antiferromagnets," *ACS Applied Electronic Materials,* vol. 6, no. 3, pp. 1790-1796, 2024.

[7] M. Küß, S. Glamsch, Y. Kunz, A. Hörner, M. Weiler, and M. Albrecht, "Giant surface acoustic wave nonreciprocity with low magnetoacoustic insertion loss in CoFeB/Ru/CoFeB synthetic antiferromagnets," *ACS Applied Electronic Materials,* vol. 5, no. 9, pp. 5103-5110, 2023.

[8] D. Labanowski *et al.*, "Voltage-driven, local, and efficient excitation of nitrogen-vacancy centers in diamond," (in English), *Science Advances,* ARTN eaat6574 vol. 4, no. 9, 2018.

[9] D. D. Awschalom *et al.*, "Quantum Engineering With Hybrid Magnonic Systems and Materials (Invited Paper)," *IEEE Transactions on Quantum Engineering,* vol. 2, pp. 1-36, 2021.